INL/CON-13-30856
PREPRINT

Defect annealing and thermal desorption of deuterium in low dose HFIR neutron-irradiated tungsten

21st International Conference on Plasma Surface Interactions 2014

Masashi Shimada, M. Hara, T. Otsuka, Y. Oya, Y. Hatano

May 2014

The INL is a
U.S. Department of Energy
National Laboratory
operated by
Battelle Energy Alliance

Manuscript number: P3-038 rev.1

Defect annealing and thermal desorption of deuterium in low dose HFIR neutron-irradiated tungsten

Masashi Shimada[1,*], M. Hara[2], T. Otsuka[3] Y. Oya[4], and Y. Hatano[2]

[1] *Fusion Safety Program, Idaho National Laboratory, Idaho Falls, ID, U.S.A.*

[2] *Hydrogen Isotope Research Center, University of Toyama, Toyama, Japan*

[3] *Kyushu University, Interdisciplinary Graduate School of Engineering Science, Higashi-ku, Fukuoka, Japan*

[4] *Radioscience Research Laboratory, Faculty of Science, Shizuoka University, Shizuoka, Japan*

Abstract –

Three tungsten samples irradiated at High Flux Isotope Reactor at Oak Ridge National Laboratory were exposed to deuterium plasma (ion fluence of $1x10^{26}$ m^{-2}) at three different temperatures (100, 200, and 500 °C) in Tritium Plasma Experiment at Idaho National Laboratory. Subsequently, thermal desorption spectroscopy was performed with a ramp rate of 10 °C min^{-1} up to 900 °C, and the samples were annealed at 900 °C for 0.5 hour. These procedures were repeated three times to uncover defect-annealing effects on deuterium retention. The results show that deuterium retention decreases approximately 70 % for at 500 °C after each annealing, and radiation damages were not annealed out completely even after the 3rd annealing. TMAP modeling revealed the trap concentration decreases approximately 80 % after each annealing at 900 °C for 0.5 hour.

PSI-21 keywords: Tungsten, Neutron damage, Desorption, Deuterium inventory

PACS codes: 52.40.Hf, 52.77.Dq, 61.80.-x, 68.43.Vx

*Corresponding author address: P.O. Box 1625, MS 7113, Idaho Falls, ID, 83415-7113, U.S.A.

*Corresponding author's e-mail: Masashi.Shimada@inl.gov

Presenting author: Masashi Shimada

Presenting author's e-mail: Masashi.Shimada@inl.gov

I. Introduction

Accurately estimating tritium retention in plasma facing components (PFCs) and minimizing its uncertainty are key safety issues for licensing DEMO and future fusion power reactors [1-3]. Deuterium-tritium fusion reactions produce 14 MeV neutrons that activate PFCs and create radiation defects throughout the bulk of the material of these components. Recent studies showed that tritium was trapped in bulk (>> 10 μm) tungsten beyond the detection range of nuclear reaction analysis technique [4-5], and thermal desorption spectroscopy (TDS) technique becomes the only established diagnostic that can reveal hydrogen isotope behavior in bulk (>> 10 μm) tungsten. Radiation damage and its recovery mechanisms in neutron-irradiated tungsten are still poorly understood, and neutron-irradiation data of tungsten is very limited [6]. In this paper, systematic investigation with repeated plasma exposures, thermal desorption and annealing is performed to study defect-annealing effect on thermal desorption of deuterium in low dose neutron-irradiated tungsten.

II. Experimental Apparatus

The disc-type tungsten samples (ϕ 6.0 mm x 0.2 mm) were prepared by cutting polycrystalline tungsten rod (99.99 at. % purity, from A.L.M.T. Co., Japan) annealed at 900 °C for 1 hour in a hydrogen atmosphere to relieve internal stresses in the manufacturing process. Details of the sample preparation and neutron irradiation are described elsewhere [5]. Three tungsten samples were irradiated by neutrons in the High Flux Isotope Reactor (HFIR), Oak Ridge National Laboratory at reactor coolant temperature (50-70°C) to low displacement damage of 0.025 displacement per atom (dpa) under the framework of the US-Japan TITAN program (2007-2013). The thermal neutron and fast neutron (>0.1MeV) fluxes at the irradiation location were 2.5×10^{19}, and 8.9×10^{18} $m^{-2}s^{-1}$, respectively. The thermal neutron and fast neutron (>0.1MeV) fluences for 33 hour irradiation were 3.0×10^{24} and 1.1×10^{24} m^{-2}, respectively. This fast neutron (>0.1MeV) fluence gives damage level approximately 0.025 dpa. Three 0.025 dpa tungsten samples were exposed to deuterium plasma (ion fluence of 1×10^{26} m^{-2}) at three different temperatures (100, 200, and 500 °C) in Tritium Plasma Experiment (TPE) at Idaho National Laboratory. Three non-irradiated (0 dpa) tungsten samples also were exposed to deuterium plasma at three different temperatures, and the TPE exposure and TDS

procedures were repeated (once for 100 °C, three times for 200 °C sample, and twice for 500 °C) to compare defect-annealing effects on deuterium retention in non-irradiated (0 dpa) tungsten. Details of the TPE linear plasma device and thermal desorption system are described elsewhere [7]. Since disc-type samples were prepared by cutting polycrystalline tungsten rod, a variation in the sample thickness made it challenging to obtain identical flux and temperature conditions for different thickness sample. Deuterium ion flux was varied from $0.5x10^{22}$ to $1.2x10^{22}$ $m^{-2}s^{-1}$ to keep identical exposure temperature. The recent report indicated that there exists strong dependence of ion fluence on tritium retention and less dependence of ion flux [8]. Therefore, the ion fluences in each TPE plasma exposure were kept approximately $1x10^{26}$ m^{-2} as shown in table 1. Subsequently, thermal desorption spectroscopy (TDS) was performed with a ramp rate of 10 °C/min up to 900 °C, and then the samples were annealed at 900 °C for 0.5 hour at the end of the TDS. These procedures were repeated to uncover defect-annealing mechanisms and its effects on deuterium retention. These samples were used for previous nuclear reaction analysis (NRA) study [4-5, 9] and the time interval between plasma exposure at TPE and TDS were approximately 600 days for the non-anneal sample due to radioactive material handling and shipping to/from NRA facility. For the 1^{st}, 2^{nd}, and 3^{rd} annealed sample, the time interval between plasma exposure at TPE and TDS were kept identical at 19 hours. Therefore, near surface deuterium in the non-annealed sample (especially 100 and 200 °C) might have desorbed during this 600 days time interval due to isotope exchange with hydrogen. In this study we denote the samples performed no TDS and no annealing after neutron-irradiation prior to TPE exposure as “no-anneal”, the samples performed one TDS and one annealing prior to TPE exposure as “after 1^{st} anneal”, the samples performed two TDS and two annealing prior to TPE exposure as “after 2^{nd} anneal”, and the samples performed three TDS and three annealing prior to TPE exposure as “after 3^{rd} anneal”. Positron annihilation spectroscopy confirmed the exposure temperatures of < 500 °C have little effects in defect recovery compared with the annealing temperature of 900 °C [10].

III. Numerical Analysis

TMAP (Tritium Migration Analysis Program) was developed by fusion safety program, INL in 1980’s to dynamically analyze dissolved gas movement through structure, between structures and

adjoining enclosures, and among enclosures for safety analysis purpose. TMAP has application to a much wider variety of problems, and has been widely used in the PFC community to simulate hydrogen isotope behavior in the PFCs [11-12]. A recent extension of the TMAP trap-site model was successfully carried out in the version 4 (TMAP4) to include as many traps as required by the user to simulate retention of tritium in neutron damaged tungsten material [13]. Details of the TMAP simulation and mass transport property used in tungsten are described elsewhere [9, 13]. In this study the enhanced diffusion zone (EDZ) model that Venhaus and Causey simulated tritium plasma implantation was used to simulate both plasma exposure phase and thermal desorption phase in order to accurately elucidate deuterium behavior in neutron-irradiated tungsten [14-17]. Experimental sample transfer procedure in air from the TPE vacuum chamber to the TDS vacuum chamber was not simulated, and the sample were assumed to be in vacuum at room temperature for 19 hours from the end of plasma exposure to the beginning of TDS instead. Venhaus and Causey adjusted the diffusivity in the EDZ from 5.0×10^{-10} to 2.0×10^{-9} m^2/s to fit experimental data. In this paper we utilized the EDZ in ion implantation zone (<10 nm), and varies the deuterium diffusivity in the similar range from 0.9×10^{-10} to 5.0×10^{-10} m^2/s to fit experimental data. Deuterium implantation profile (100 eV D^+ in W) obtained from the SRIM code with the displacement energy of 90 eV was used for this simulation [18]. Hydrogen diffusivity formula (corrected for deuterium) by Frauenfelder was used in normal diffusion zone (NDZ), which is beyond 10 nm from surface [19]. Recombination coefficients vary by several orders of magnitude in the literature, and the recombination coefficient formula by Anderl at al [20] ($K_r = 3.2 \times 10^{-15} \exp(-1.16 eV/kT)$ [m^4/s]) was used. This recombination coefficient is high enough to treat surface deuterium concentration to zero; therefore, we treat the surface deuterium concentration to be zero as a boundary condition in this simulation as suggested by Causey et.al. [14-16]. Uniform distribution of empty traps with user specified concentration is introduced first, and the deuterium plasma exposure is simulated with similar deuterium ion flux and temperature profile obtained experimentally to investigate deuterium behavior (e.g. how deep deuterium atoms migrate and trap) in tungsten. Then, the thermal desorption phase were simulated with the ramp-rate of 0.167 °C s^{-1} (= 10 °C min^{-1}) and the maximum temperature of 900 °C. There are three types of fitting parameters in this modeling. The diffusivity in the EDZ determines deuterium solution concentration

117 penetrating into the NDZ; therefore it governs how deep deuterium atom can migrate with given trap
118 concentration and detrapping energy. Effective diffusivity decreases as the trap concentration and
119 detrapping energy increase. In general, the first fitting parameter, detrapping energy, can be
120 determined by the TDS peak positions, and the second fitting parameter, trap concentration, can be
121 obtained by the maximum deuterium flux (peak height) of TDS peak. Two detrapping energies of
122 1.25(±0.15) eV and 1.70(±0.10) eV were used in this study. Uniform trap concentration throughout
123 sample thickness was used for simplicity and due to unavailability of deuterium depth profile
124 diagnostic in bulk W (> 5 μm). The third fitting parameter, diffusivity in the EDZ, can be acquired
125 from the shape (width) of TDS peak.
126
127 **IV. Results and Discussion**
128 According to the review of defect recovery in tungsten [6], the stage III recovery, which is
129 attributed to the migration of mono-vacancies, was observed around 300-400 °C, and the migration
130 energy of mono-vacancy were reported to be approximately 1.7 eV. For the sample exposed at 100
131 and 200 °C, the sample temperature was kept below the stage III recovery temperature to prevent
132 defect recovery during the deuterium plasma exposure, and the effect of diffusion on the deuterium
133 depth profile is evaluated. In fact the TDS spectra of 100 °C exposure are very similar to that of
134 200 °C exposure. Almost all the deuterium atoms were desorbed or isotope-exchanged hydrogen in
135 the non-annealed 100 °C exposed sample during the long time interval (~ 600 days) between plasma
136 exposure and TDS for the non-anneal sample, and it showed negligibly small deuterium retention,
137 making it difficult to compare with annealed results. For the sample exposed at 500 °C, the sample
138 temperature was above the stage III recovery temperature, and the effects of the stage III recovery on
139 deuterium retention is evaluated. The stage V recovery is reported to occur slightly below 900 °C,
140 which is attributed to migration of vacancy clusters, but the size of vacancy clusters were not
141 identified in the literature [6]. Therefore; the annealing at 900 °C for 0.5 hour was chosen as annealing
142 temperature and duration to reveal the defect-annealing effects of vacancy clusters on thermal
143 desorption spectra and deuterium retention.

Figure 1 shows the thermal desorption spectra of annealed neutron-irradiated tungsten samples exposed to the ion fluence of $1x10^{26}$ m^{-2} at (a) 200 °C and (b) 500 °C. For 200 °C case, Figure 1a shows similar profiles with two distinctive peaks: a low temperature peak located around 250-350 °C, and a high temperature peak located around 500-600 °C. The maximum deuterium desorption flux increased from "no-anneal" to "after 1st anneal". It is important to note that only the low temperature peak located around 250-350 °C was observed from the non-irradiated (0 dpa) 200 °C sample (not shown) and there was no distinctive change in deuterium retention due to annealing. For 500 °C case, Figure 1b shows similar profiles with one distinctive peak located different temperature around 750-850 °C for "no-anneal" and 500-600 °C for the sample after 1st, 2nd, and 3rd anneal. Negligible small deuterium retention below $9.0x10^{16}$ m^{-2} was observed from the non-irradiated (0 dpa) 500 °C sample (not shown) and there was no distinctive change in deuterium retention due to annealing. It is interesting to note that figure 1b (500 °C case) showed consistent trend in thermal desorption behavior after 1st, 2nd, and 3rd anneal, but figure 1a (200 °C case) did not show any trend after 1st, 2nd, and 3rd anneal. Near surface retention (< a few μm) is the major contributor to deuterium retention in 200 °C results, whereas bulk retention (>> 10 μm) predominates deuterium retention in 500 °C results. Deuterium irradiation effect (from high-flux plasma) can not be distinguished with neutron (or high-energy ion) irradiated damage at near surface (< a few μm) since high solution concentration of deuterium atoms in tungsten lattice creates additional ion-induced damage and trap site such as bubble or blister formations, making it challenging to understand defect recovery at near surface (for the 200 °C case) when trapped deuterium atoms are used as a defect detector. The different behavior can be attributed to bubble or blister formations at near surface. Further investigation with transmission electron microscopy and positron annihilation spectroscopy is necessary to reveal different behavior in defect recovery between 200 °C and 500 °C. Figure 2 shows defect-annealing effects on (a) deuterium retention obtained experimentally via TDS and (b) trap concentration obtained numerically via TMAP at two different plasma exposure temperatures (200 and 500 °C). Deuterium retention was obtained by integrating deuterium desorption flux in the TDS spectrum in Figure 1. Trap concentration was obtained by fitting experimental TDS spectrum with detrapping energy in TMAP. Detrapping energy was also obtained by TMAP, and it is interesting to note that the detrapping energy

of 500 °C changes from 1.75 to 1.6 eV at the 1st annealing. This could be defect structure change due to migration of vacancy cluster to form larger vacancy cluster or voids. Note that near surface deuterium retention of non-annealed 200 °C sample was underestimated since thermal desorption of non-annealed samples were performed in approximately 600 day after plasma exposure. However, this long time interval has minimal effects on bulk deuterium retention of non-annealed 500 °C sample; therefore, it shows consistent defect-annealing trends. Figure 2a shows that the deuterium retention decreases approximately 70 % for at 500 °C after each annealing, all the radiation damage was not annealed out completely even after the 3rd annealing. Deuterium retention is a function of various factors (e.g. plasma ion flux, exposure temperature, plasma duration, trap concentration, and detrapping energy), and trap concentration is more suited for investigating defect-annealing effects. In the simplified picture, deuterium retention is product of deuterium concentration and deuterium penetration depth, and deuterium diffusion determines this deuterium penetration depth. Presence of trap site has significant effect on deuterium diffusion [4, 21]. According to Oriani [21], the effective diffusivity D_{eff} under trapping effects can be written as $D_{eff} = D_L/(1 + \exp(E_{bin}/kT)\, C_t/C_L)$, where D_L is the diffusion coefficient of H in a normal lattice of W, C_t is the trap concentration, C_L is the concentration of interstitial sites, and E_{bin} is the binding energy. Figure 2b shows that the trap concentration obtained from TMAP modeling decreases approximately 80 % for 900°C exposure sample after each annealing at 900 °C for 0.5 hour, indicating that deuterium atom was migrated slightly deeper after each annealing due to slight increase in effective diffusivity as the trap concentration decreases.

V. Conclusions

Three HFIR neutron-irradiated tungsten samples were exposed to deuterium plasma (ion fluence of 1×10^{26} m^{-2}) at three different temperatures (100, 200, and 500 °C) in TPE, and TDS was performed with a ramp-rate of 10 °C min^{-1} up to 900 °C and an annealing at 900 °C for 0.5 hour. These procedures were repeated to uncover defect-annealing effects on deuterium retention. The results show that deuterium retention decreases approximately 70 % for at 500 °C after each annealing, and all the radiation damage was not annealed out completely even after the 3rd annealing. TMAP

200 modeling revealed the trap concentration decreases approximately 80 % after each annealing at
201 900 °C for 0.5 hour.
202
203 **VI. Acknowledgements**
204 This work was prepared for the U.S. Department of Energy, Office of Fusion Energy Sciences,
205 under the DOE Idaho Field Office contract number DE-AC07-05ID14517.

VII. References

[1] N. Taylor, D. Baker, S. Ciattaglia, P. Cortes, J. Elbez-Uzan, M. Iseli, S. Reyes, L. Rodriguez-Rodrigo, S. Rosanvallon, L Topilski, *Fus. Eng. Des*. **86** (2011) 619

[2] N. Taylor, S. Ciattaglia, P. Cortes, M. Iseli, S. Rosanvallon, and L. Topilski, *Fus. Eng. Des*. **87** (2012) 476

[3] N. Taylor, C. Alejaldre, and P. Cortes, *Fus. Sci. Technol.* **64** (2013) 111

[4] Y. Hatano, M. Shimada, V.Kh. Alimov, J. Shi, M. Hara, T. Nozaki, Y. Oya, M. Kobayashi, K. Okuno, T. Oda, G. Cao, N. Yoshida, N. Futagami, K. Sugiyama, J. Roth, B. Tyburska-Püschel, J. Dorner, I. Takagi, M. Hatakeyama, H. Kurishita, and M.A. Sokolov*, J. Nucl. Mater.* **438** (2013) S114-S119

[5] Y. Hatano, M. Shimada, T. Otsuka, Y. Oya, V.Kh. Alimov, M. Hara, J. Shi, M. Kobayashi, T. Oda, G. Cao, K. Okuno, T. Tanaka, K. Sugiyama, J. Roth, B. Tyburska-Püschel, J. Dorner, N. Yoshida, N. Futagami, H. Watanabe, M. Hatakeyama, H. Kurishita, M.A. Sokolov, and Y. Katoh*, Nucl. Fusion* **53** (2013) 073006

[6] H. Schultz, "*The Landolt-Börnstein Database* (http://www.springermaterials.com)" volume III/25 "*Atomic Defects in Metals*" (Springer Materials 1991), ed Ullmaier H, section 2.2.3. DOI: 10.1007/10011948_54

[7] M. Shimada, R. D. Kolasinski, J. P. Sharpe, and R. A. Causey, *Rev. Sci. Instrum.* **82** (2011) 083503.

[8] B. Lipschultz, J. Roth, J.W. Davis, R.P. Doerner, A.A. Haasz, A. Kalenbach, A. Kirschner, R.D. Kolasinski, A. Loarte, V. Philipps, K. Schmid, W.R. Wampler, G.M. Wright, and D.G. Whyte, *"An assessment of the current data affecting tritium retention and its use to project towards T retention in ITER", MIT Report* PSFC/RR-10-4, 2010

[9] M. Shimada, G. Cao, Y. Hatano, T. Oda, Y. Oya, M. Hara, and P. Calderoni, *Phys. Scr.* **T145** (2011) 014051

[10] C.N. Taylor, M. Shimada, B.J. Merrill, D.W. Akers, Y. Hatano, *submitted to J. Nucl. Mater. this special issue*

[11] G.R. Longhurst, D.F. Holland, J.L. Jones, and B.J. Merrill, "*TMAP4 User's Manual"*, Idaho National Laboratory, EGG-FSP-10315 (1992)

[12] G.R. Longhurst, "*TMAP7: Tritium Migration Analysis Program*," User Manual, Idaho National Laboratory, INEEL/EXT-04–02352, Rev. 2 (2008)

[13] B.J. Merrill, M. Shimada, and P.W. Humrickhouse, *J. Plasm. Fus. Res. SERIES*, **10** (2013) 71

[14] R.A. Causey, K. Wilson, T. Venhaus, and W.R. Wampler, *J. Nucl. Mater.* **266-269** (1999) 467-471

[15] T. Venhaus, R.A. Causey, R.P. Doerner, and T. Abeln, *J. Nucl. Mater.* **290-293** (2001) 505-508

[16] T. Venhaus, and R.A. Causey, *Fusion Technology*, **39 (**2001), 868-873

[17] M. Shimada, G. Cao, T. Otsuka, M. Hara, M. Kobayashi, Y. Oya, and Y. Hatano, *submitted to Nuclear Fusion*.

[18] Stopping and Range of Ions in Matter (SRIM), J.F. Ziegler, http://www.srim.org

[19] R. Frauenfelder*, J. Vac. Sci. Technol.* **6** (1969) 388

[20] R.A. Anderl, D.F. Holland, G.R. Longhurst, R.J. Pawelko, C.L. Trybus, and C.H. Sellers, *Fusion Technol.* **21** (1992) 745

[21] R.A. Ariani, *Acta Metall.* **18** (1970) 147

Tables

Table 1. The experimental (HFIR irradiation[a] and TPE plasma[b]) conditions.

Sample ID	Weight [gram]	Sample size[c] (diameter / thickness) [mm]	HFIR irradiation dose [dpa]	TPE exposure temperature [°C]	Ion fluence[d] [m^{-2}]			
					no-anneal[g]	after 1st anneal[g]	after 2nd anneal[g]	after 3rd anneal[g]
Y102	0.80	6.0 / 0.15	0.025	100	1.0E+26	1.0E+26	6.3E+25[f]	4.2E+25[f]
Y103	0.89	6.0 / 0.16	0.025	200	9.7E+25	1.0E+26	1.0E+26	9.8E+25
Y105	0.83	6.0 / 0.15	0.025	500	1.2E+26	1.0E+26	6.1E+25[f]	9.8E+25

[a] HFIR irradiation temperature was at the reactor coolant temperature of 50-70 °C

[b] Incident ion energy was approximately 100 eV for all samples.

[c, d] Sample thickness varies due to slicing 6 mm diameter tungsten rod. This variation in the sample thickness made it challenging to obtain identical flux and temperature conditions for different thickness sample. The ion fluences in each TPE plasma exposure were kept approximately $1x10^{26}$ m^{-2}, for each sample.

[f] Desired ion fluences ($1x10^{26}$ m^{-2}) were not achieved due to poor plasma performances and plasma fluctuations.

[g] We denote the samples that performed no TDS and no annealing after neutron-irradiation as "no-anneal", the samples performed one TDS and one annealing as "after 1st anneal", the samples performed two TDS and two annealing as "after 2nd anneal", and the samples performed three TDS and three annealing as "after 3rd anneal".

[table width: two column]

Figures

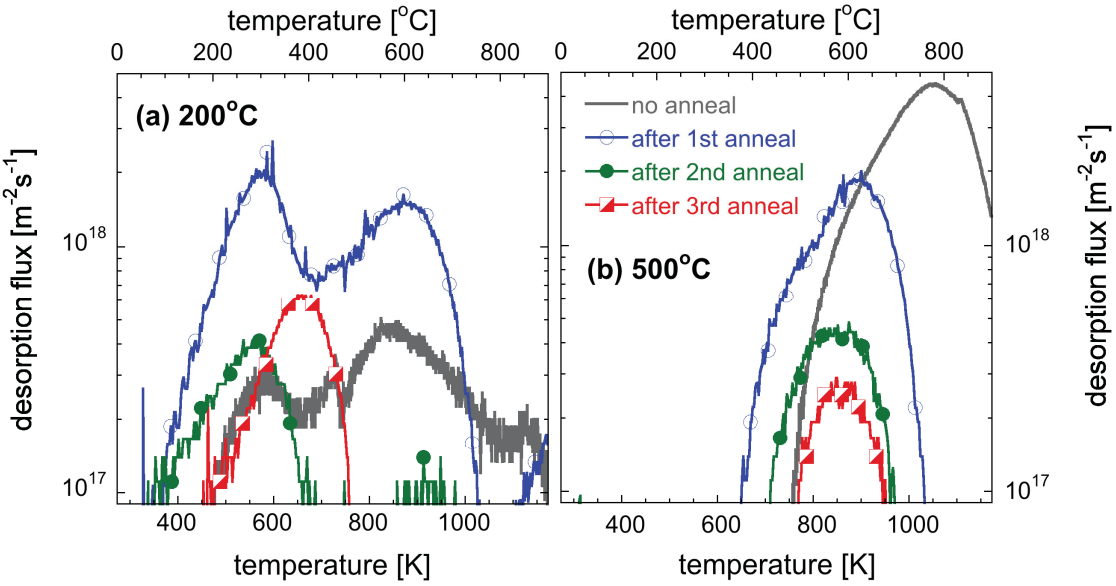

Fig. 1: Thermal desorption spectra of annealed neutron-irradiated tungsten samples exposed to the total ion fluence of 1×10^{26} m^{-2} at (a) 200 °C and (b) 500 °C. Solid line denotes for no anneal, line with open circle denotes for after 1st anneal, line with solid circle denotes for after 2nd anneal, and line with square denotes after 3rd anneal.

[figure width: two column (160 mm) , height: 85 mm, color, filename: “Shimada PSI2014 Fig1.tif”]

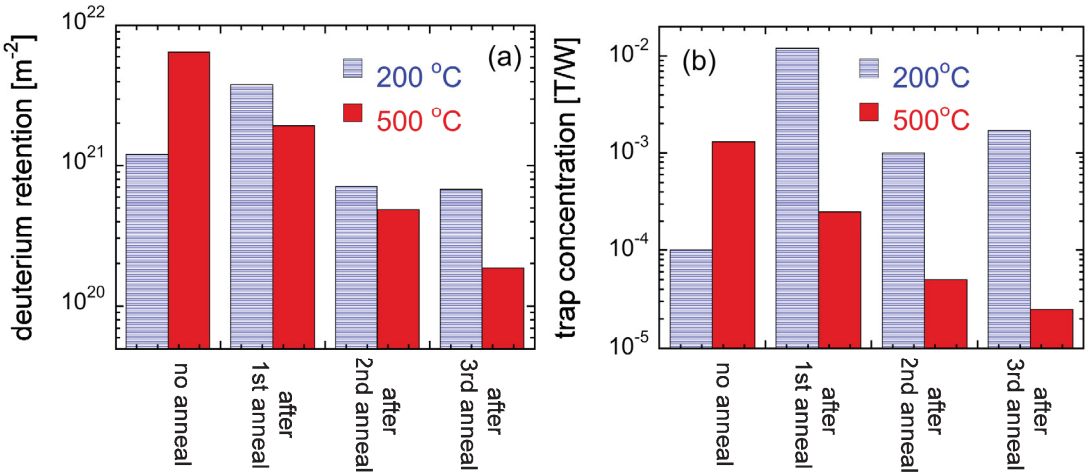

Fig. 2: Defect annealing effects on (a) deuterium retention obtained experimentally via TDS and (b) trap concentration obtained numerically via TMAP at two different plasma exposure temperatures (200, and 500 °C).

[figure width: two column (160 mm) , height: 71 mm, color, filename: “Shimada PSI2014 Fig2.tif”]